SCALE-UP OF PHOTOCATALYSIS-ASSISTED WATER DISINFECTION:

OPPORTUNITIES AND BARRIERS

A Thesis

by

JONATHAN ALEX BOCKENSTEDT

Submitted to the Graduate and Professional School of
Texas A&M University
in partial fulfillment of the requirements for the degree of

MASTER OF SCIENCE

Chair of Committee,	Sreeram Vaddiraju
Committee Members,	Terry Gentry
	Hung-Jen Wu
Head of Department,	Arul Jayaraman

December 2021

Major Subject: Chemical Engineering

ABSTRACT

Dwindling supplies of readily available freshwater, coupled with the continuous growth of the human population, necessitates the purification and reuse of wastewater. This requires next-generation treatment processes, such as advanced oxidative processes (AOPs, e.g., photocatalysis), that offer the ability to remove both harmful microorganisms and other contaminants of emerging concern (CECs) from water. Building upon the laboratory-scale successes of AOPs for the large-scale remediation of water, however, requires process development. To accomplish this goal, a custom-built mobile platform capable of processing 15.14 liters (4 gallons) per minute of water is built and employed for studying the photocatalytic inactivation of *Escherichia coli* (*E. coli*) from water. This study indicated that the benchtop setup is as efficient as laboratory-scale studies in disinfecting water by photocatalysis. The study also indicated that catalyst recovery, regeneration and reuse is possible via a combination of gravity-assisted settling, centrifugation and air plasma treatment of the recovered photocatalysts.

ACKNOWLEDGEMENTS

I would like to thank my committee chair, Dr. Vaddiraju, for giving me the opportunity to make this work possible. His guidance throughout the course of this project was invaluable, and he taught me what it meant to take pride in my research. I would also like to thank my committee members, Dr. Gentry and Dr. Wu, for letting my defense be an enjoyable moment and for providing their comments.

In addition, I would like to thank Niraj for working with me for the past 4 years, back to when I was still an undergraduate. His advice and help with all the experiments, failed or successful, made this possible.

Thanks also goes out to all my friends throughout the department for making my time at Texas A&M a great experience.

Finally, thanks to my parents and family for their support throughout my time at university.

CONTRIBUTORS AND FUNDING SOURCES

Contributors

This work was supervised by a thesis committee consisting of Professor Sreeram Vaddiraju and Professor Hung-Jen Wu of the Department of Chemical Engineering and Professor Terry Gentry of the Department of Soil and Crop Sciences.

Funding Sources

This research was partially funded by Agriculture and Food Research Initiative Competitive Grant no. 2018-67016-27578 awarded as a Center of Excellence from the USDA National Institute of Food and Agriculture. This project was also partially supported by the Research, Engineering and Extension: Creation and Deployment of Water-Use Efficient Technology Platforms “Water Seed Grant Initiative” by Texas A&M University System.

TABLE OF CONTENTS

Page

LIST OF FIGURES

Page

1. INTRODUCTION AND BACKGROUND

Water is one of the most important natural resources for life. To live, humans require water, air, and food. Although they are listed separately, water plays an essential role in our food and oxygen supply. Plants require water to live and, in turn, produce oxygen during photosynthesis. Agriculture practitioners cultivate a subset of these plants, called crops, on a large-scale to facilitate our food supply.

Although it appears that water is abundantly available as it covers over 70% of the earth, only around 3% of the total amount of water available is fit for human consumption. Of this 3%, only 1% is readily available as the other 2/3 is frozen in polar ice caps and glaciers. The remaining 97% is seawater, which is too saline for human consumption or irrigation. Another important item to note is that the total quantity of water on earth is, for all intents and purposes, constant. Our water reservoir has been recycled countless times through the water cycle [1].

A major problem mankind is currently facing is the continuous growth of the human population. This is putting greater demand on the supply of water. In *Water*, Marq De Villiers [2] states, “Humans consume water, discard it, poison it, waste it, and restlessly change the hydrological cycles, … The human population is burgeoning, but water demand is increasing twice as fast.” Realizing that Earth has a finite amount of water available, but an ever-increasing demand, we must understand that we need to find new ways to produce clean water. One method of doing so is the purification and reuse of water that would normally be treated as wastewater.

Focusing specifically on irrigation, in 2015 irrigation withdrawals were 118 billion gallons per day [3]. These withdrawals, all freshwater, accounted for 42% of freshwater withdrawals in 2015. The use of reclaimed wastewater as a source of irrigation water was also reported in 10 States (California, Florida, Arizona, Texas, Utah, Nevada, New Mexico, Colorado, Kansas, and Illinois) and accounted for 669 million gallons per day, or less than 1% of total irrigation water used [3]. To combat the increasing demand on our water supply, the amount of reclaimed wastewater used in irrigation needs to increase.

The process for remedying wastewater to meet quality requirements for irrigation needs depends on the quality of the wastewater source. In general, surface water requires more process steps than groundwater to transform the raw source water into a usable final product. The major unit operations that make up standard water treatment processes are screening, coagulation, flocculation, sedimentation, filtration, disinfection, and distribution [1]. This subsequent discussion will be limited to methods employed for disinfecting water, as this is the topic of the current work.

1.1. Current Methods of Water Disinfection

Disinfection is a process that works to inactivate recognized pathogenic microorganisms. It can be split into two categories: primary disinfection and secondary disinfection. Primary disinfection initially kills the bacteria/cyst/virus. Secondary disinfection is the use of a disinfection residual that will prevent the regrowth of microorganisms once the primary disinfection has ended [1]. Current wastewater treatment practices disinfection to a point where enough of the disease-causing agents are

eliminated to protect public health; however, this does not mean all microbial life within the water is eliminated. Some examples of popular methods of disinfection used today are chlorination, ozonation, and ultraviolet (UV) radiation. In the following sections, these current state-of-the-art technologies for water disinfection are discussed in the context of their advantages and drawbacks. In addition to the state-of-the-art technologies, photocatalysis is also described in detail in the following section.

1.1.1. Chlorination

The chlorination process involves the addition of various forms of chlorine to water, gaseous chlorine, sodium hypochlorite, and calcium hypochlorite being some of the examples. These forms of chlorine react with various substances or impurities within the water, forming hypochlorous acid and hypochlorite ions [4]. Hypochlorous acid and hypochlorite ions are oxidizers and are the disinfection agents associated with chlorination.

Chlorine and the chlorine-containing compounds are inexpensive and commercially available, making chlorination cost-effective and scalable. Chlorination has been around for over a century, so it is well established, refined and efficient. It also has the potential to offer residual disinfection if the dosage of chlorine is large enough [4], [5].

On the other hand, some of the disinfection by-products (DBPs) associated with chlorination are harmful, in particular, the carcinogenic group of trihalomethanes which are formed when organic compounds within the water react with chlorine [4], [5], [6], [7]. Also, some protozoans have been shown to be resistant to chlorination [5]. An example of

this being a problem can be seen in the 1993 Milwaukee Cryptosporidiosis outbreak [8]. An ineffective filtration system resulted in *Cryptosporidium* persisting through the water-treatment plants and the chlorine disinfection method was unable to remedy the wastewater, resulting in the death of 69 people.

1.1.2. Ozonation

Similar to chlorination, ozonation is a chemical disinfection process; however, instead of the addition of chlorine, ozonation involves the use of ozone as the oxidizer. When ozone decomposes in water, the free radicals hydrogen peroxy and hydroxyl are formed. These free radicals are great oxidizers and are believed to play the primary role in the disinfection process through protoplasmic oxidation which results in cell wall disintegration [9], [10], [11].

Ozone has greater germicidal abilities than those of chlorine, meaning that it is more effective than chlorine in destroying bacteria and viruses [9]. In bromide-free waters, there are no DBPs associated with the ozonation process [12], [13], [14]. In addition, there are no harmful residuals that need to be removed after ozonation as it decomposes rapidly [9].

Ozonation is a more complex technology than UV radiation or chlorination. When coupled with the requirement to generate ozone on site due to its rapidly decomposing nature, the capital costs associated with this method are greatly increased. Also due to its rapid decomposition rate, ozone also provides no secondary disinfection [9], [4]. To

prevent contamination, another residual disinfectant, such as chlorine or iodine, must be added if the disinfected water is to be stored for a long duration.

1.1.3. UV Disinfection

UV disinfection utilizes the high-energy photons associated with UV-C radiation to inactivate microbes through the disruption of their DNA. The nucleic acids, RNA and DNA, absorb the energy from the radiation and form new bonds between adjacent nucleotides. The dimerization of these nucleotides causes the DNA to mutate, inactivating the microbe [15], [16], [17], [18].

As opposed to chlorination and ozonation, UV disinfection is a physical process, not a chemical process which is a large advantage over the other two disinfectants [1]. With its requirement of only a UV light source, this physical process eliminates the need for storage or handling of potentially toxic materials [15]. UV disinfection does not form enough DBPs to pose a problem [18]. Finally, UV disinfection will also inactivate chlorine-resistant pathogens like *Cryptosporidium* [15].

Although very effective at combating microbes, UV disinfection is heavily reliant on the incoming water quality. In order for the microorganisms to be properly inactivated, the appropriate amount of UV radiation needs to reach them [15]. Pre-treatment of the water supply is necessary if the turbidity of the incoming water would be enough to block the necessary UV Transmittance (UVT) levels for inactivation. One of the major disadvantages to using UV radiation for disinfection is the lack of secondary, or residual,

disinfection [15], [18]. Similar to ozonation, another residual disinfection must be added if the water is to be stored for a long duration.

1.2. Photocatalytic UV Disinfection

Photocatalysis is another, less popular, method of disinfection. Photocatalysis utilizes the energy from UV radiation, but in the presence of a catalyst which accelerates the photoreaction. In the titanium dioxide (TiO_2)-catalyzed disinfection of water, the irradiation of the semiconductor generates the reactive oxidant species (ROS) [19], [20], [21], [22], [23]. The actual mechanism for cell death is not completely settled, but the prevailing theory is that the pathogen inactivation mechanism is owed to membrane and cell wall damage [20], [21]. The ROS attack the external membrane of the cell, either changing its permeability or destroying it. The ROS then reaches the cell wall and cytoplasmic membrane, causing lysis of the cell.

This technology has the added benefit of the catalyst being reusable, at least in theory, after disinfection. The catalyst can be filtered out of the treated wastewater, regenerated, and used again in photocatalysis. Photocatalysis can also occur at lower wavelengths of light than traditional UV disinfection. Due to the band gap energy of anatase, around 3.2 eV, photocatalysis can be utilized using light with wavelengths below 385 nm [21]. Finally, photocatalysis could be used to remove emerging contaminants that are otherwise difficult to remove by membrane-assisted filtration processes, including fertilizers, per-fluoroalkyl substances, and pharmaceuticals [24], [25]. Therefore, this

work is aimed at studying UV-A-assisted photocatalysis for disinfecting large quantities of water. Similar to UV radiation, photocatalysis does not have residual disinfection in the traditional sense. This can be alleviated by storing the treated wastewater in a UV transparent storage vessel in direct sunlight. All UV-C radiation and approximately 90% of UV-B radiation from sunlight are absorbed the atmosphere [26]. As a result, most of the UV radiation reaching the Earth's surface is UV-A. This storage method will allow for continuous disinfection during storage at no additional costs.

The water treated by photocatalysis does need to have the photocatalyst filtered out before consumption. With our current technology, this poses problems as filtering out the nanomaterials to the levels of safe consumption is difficult for large-scale processes. Similar to UV radiation, photocatalysis requires pre-treatment of the water to appropriate UVT levels for inactivation [15].

2. CONSTRUCTION OF LARGE-SCALE DISINFECTION UNIT

2.1. Design Parameters

The construction of a large-scale portable disinfection unit allowed for three apects to be addressed: the identification of problems associated with the scale-up of photocatalysis process for water disinfection, the exploration of new opportunities that arise when operating on a larger scale, and the ability to deploy and demonstrate the unit to stakeholders (e.g., farmers, food producers and processors). To properly address these aspects, certain design criteria were defined before construction of the water disinfection system.

- Portability/Mobility: Of primary importance in the design of the unit is its portability/mobility. To be able to demonstrate the capabilities of the unit to stakeholders requires the unit be safely and easily transportable.
- Inlet filtration: Photocatalytic disinfection kinetics are a function of the inlet water quality. To ensure the disinfection process proceeds favorably, inlet water filtration is necessary. This makes the system versatile for use with a type and source of inlet water.
- Sensors assessing/quantifying water quality: Working together with the aforementioned design parameter, portable sensors for continuous monitoring of the water quality are necessary to ensure the water quality is within acceptable standards for photocatalytic disinfection.

- Catalyst introduction: As this disinfection unit functions like a testbed to understand the kinetics of large-scale photocatalytic disinfection, there needs to be a way to introduce the chosen catalyst, after the filtration of the incoming water.
- Sampling: The collection of samples throughout the course of an experiment is necessary, so an avenue for easy sampling should be available.
- Ability to handle large volumes of water: One of the purposes of this unit is to demonstrate the viability of photocatalytic disinfection on a larger scale. This requires that the unit be able to handle water volumes much higher than those used in small-scale experiments (i.e., in static beaker-and-bottle experimentation).

2.2. Components

The intent of ensuring the unit could be fabricated and deployed for any of the stakeholders led to the use of only commercially available components in the construction of the water disinfection system. When choosing the tubing to construct the flow system, the primary considerations were that the system must be leak-proof and easy to assemble/alter/disassemble. The continuous loop flow system was designed using Swagelok® 3/8” diameter stainless steel pipe. The Swagelok® tubing was connected to other parts of the setup using national pipe thread (NPT) connections. Along with the piping, this flow system was made up of the following components: a series of commercially-available water filters (GE® water filters) for pre-treatment of incoming water, an inlet tank (TAMCO® Industries) equipped with an electronic overhead mechanical stirrer (Velp Scientific Inc.) for continuous mixing of the water and

photocatalyst, a commercially-available UV water disinfection system (Atlantic Ultraviolet Corp.), a post-disinfection filter system to recover the photocatalyst from the treated water (GE® water filters), and an outlet tank for holding the disinfected water (TAMCO® Industries). In addition to these components, two 250 gph magnetic drive utility pumps (Danner Manufacturing Inc.) were added to the system to achieve a continuous flow of water. Finally, a multiparameter pH/ISE/EC/DO/turbidity waterproof meter (Hanna Instruments) is also included with the system for continuously monitoring both inlet and outlet water qualities.

The type of pre-treatment filters used in the flow system may be changed depending on the quality of the inlet water. The use of GE® filter housings allows for numerous types of GE® filters to be interchanged into the system easily, giving greater filtration capabilities due to the wide variety of GE® filters available. The current iteration of the system uses three filters operating in series for pre-treatment. These filters include a 5-micron sediment filter, a 5-micron granular activated carbon filter, and a 5-micron CTO (chlorine, taste, and odor) carbon block filter. These three filters were chosen as they are commonly used in most reverse osmosis (RO) systems.

The inlet and outlet tank needed to be tall, narrow, and open top containers. Tall and narrow tanks will allow us to process less water for each experiment as these types of tanks require less volume to reach the water level at the height of the outlet than shorter, wider tanks would. This is especially useful for laboratory-scale studies. Open-top tanks also allow for their thorough cleaning after every experiment. This is important as when

testing the efficacies of different photocatalysts, prevention of photocatalyst cross-contamination requires thorough cleaning of the unit between experiments.

The UV purifier (Atlantic Ultraviolet Corp.) chosen processes 15.14 liters (4 gallons) per minute and provides high exposure to the UV lamp within. The purifier initially comes with a UVC lamp encased within a quartz tube that spans the length of the purifier; however, the lamp is removable. For certain experiments, the UVC lamp was removed and replaced with UVA LEDs (365 nm, Waveform Lighting).

The design requirements for the pumps are that they operate in-line and pump at least 15.14 liters per minute due to the chosen UV purifier. The currently flow system has two identical 250-gph magnetic drive water pumps (Danner Manufacturing Inc.) operating independently from one another to allow for continuous flow of water throughout the entire system. One pump is used solely for the recycle stream (Figure 1).

In addition to these, each and every component of the unit is equipped with valves and bypasses to make it easy to add or bypass any required step (e.g., inlet water filtration, outlet water filtration). This is essential for cycling water continuously through the process multiple times to adjust the photocatalysis process residence time and thereby study the kinetics of the photocatalytic disinfection process. Sample ports are located throughout the unit to give easy access to sampling, regardless of the orientation the unit is being operated in (Figure 1).

A standalone portable equipment kit based on BactiQuant® water technology was added to the unit to aid in the rapid quantification of bacteria in water (Mycometer). This

addition offers order of magnitude analysis of concentration in short time frames (30 minutes – 1 hour).

The entire flow system and all the associated components were mounted on a mobile platform made by connecting two dollies and a supportive base to add both mobility and portability to the unit. This allows for easy deployment of the unit on the field for demonstration of the photocatalysis process to stakeholders (Figure 1) [27].

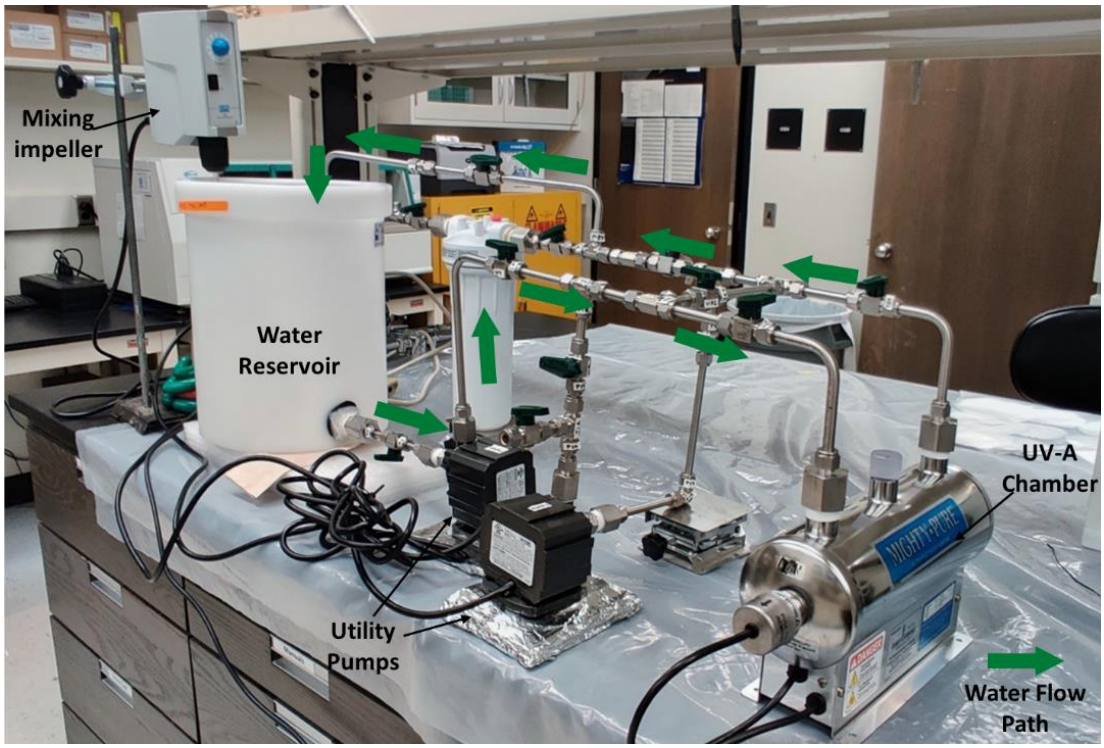

Figure 1 - A picture of the benchtop water disinfection system built for processing 15.14 liters (4 gallons) of water per minute. The setup could also be mounted on a mobile stand for onsite disinfection of water at any desired location. Reprinted with permission from [27].

3. EXPERIMENTAL METHODS*

3.1. Microorganism Growth for Large-Scale Experiments

Aliquots of *Escherichia coli* (ATCC® 51739™) preserved in glycerol stock at -80 °C were transferred into 250 mL of nutrient broth (LB Broth Miller) aseptically. The culture was then moved into a 37 °C incubator and slowly shaken using an orbital shaker for 18-20 hours. This suspension was centrifuged at 3000 rcf for 10 minutes. The supernatant was removed, leaving behind only the separated cells. Nanopure water was then added to the centrifuge tube containing the cells and the suspension was vortexed to wash the cells to remove any salts that might interfere with the disinfection process. The suspension was centrifuged again at 3000 rcf for 10 minutes. The cells were then washed another time using the same procedure. The supernatant of the final wash was removed and replaced with 250 mL Nanopure water and mixed, creating a resuspension of ~10^8 CFU/mL.

3.2. Plating Methodology

All samples were plated on Brain Heart Infusion Agar (Hardy Diagnostics). The plating was performed using the Eddy Jet 2W – Spiral Plater (IUL S.A.). The purpose of spiral plating is to create areas of different sample concentrations within a single plate,

* Parts of this section are reprinted with permission from Bockenstedt, J., et al., *Catalyst Recovery, Regeneration and Reuse during Large-Scale Disinfection of Water Using Photocatalysis.* Water, 2021. **13**(19).

resulting in one plate containing the equivalent of a threefold decimal dilution concentration range. This is done by rotating the agar plate while pouring decreasing amounts of liquid onto the surface. For almost all samples, the spiral plater was operated in the Log Mode 50 µL specification. In this mode, 50 µL of sample is poured onto the plate while the volume poured across each section of the plate decreases logarithmically. Plated samples were placed inside a 35 °C incubator for at least 18 hours before being removed and enumerated. All samples were enumerated using the IUL SphereFlash® automatic colony counter and exported into Microsoft Excel.

3.3. Flow Setup Orientation and Operation for Large-Scale UV-A Photocatalytic Disinfection

To study the kinetics of large-scale photocatalytic disinfection, the flow setup was operated in a streamlined orientation that only utilized the required unit operations to make the experiment possible. The inlet filter was bypassed as the samples used in the experiment consisted only of Nanopure water, resuspended bacteria, and appropriate catalyst. The use of the inlet filter would be superfluous as nothing within the sample would require pre-filtration. The outlet filter was bypassed as this experiment did not call for the removal of catalyst, and the outlet stream was fed back into the inlet tank. This created a large-scale batch process that utilized the flow setup, allowing the accurate comparison of large-scale and small-scale kinetic results.

To begin the experiment, 6.5 L of Nanopure water was added to the inlet tank, along with 700 mg of the appropriate catalyst. The suspension was mixed using an

electronic overhead mechanical stirrer (Velp Scientific Inc.) for at least 1.5 hours to allow for proper dispersion of catalyst. 500 mL of resuspended bacteria was added and mixed for another 30 minutes. A sample was taken to determine the initial concentration of the suspension. All necessary valves were opened and the main pump was turned on, creating flow throughout the system. Once proper flow was established, the UV-A (Waveform Lighting) was activated and the timer started. A sample was taken every 30 minutes. This procedure was followed for the UV-A control experiments, except those trials omitted the addition of photocatalyst and consequently the initial mixing period. After the single-use UV-A photocatalytic disinfection experimenters were performed, the 7 L of wastewater was collected and autoclaved for 1 hour at 121 °C to kill any remaining bacteria.

3.4. Recovery, Regeneration, and Characterization of Photocatalyst

After the wastewater from the UV-A photocatalytic disinfection experiments had been autoclaved, the recovery process could begin. The method chosen to separate the photocatalyst from the water was a combination of gravity settling and centrifugation. The autoclaved wastewater would be split between two 4 L polypropylene containers (VWR) and allowed to rest for at least 1 day to cool down to room temperature and provide time for the photocatalyst to settle (by gravity) and collect at the bottom of the container. After 1 day, as much excess water as possible would be decanted from the container without disturbing the sedimented photocatalyst. Once the sample volume had been decreased from 7 L to around 0.5 L, the wastewater was split between 50 mL vortex tubes (VWR) and centrifuged at 3000 rcf for 10 minutes. Most of the supernatant was removed and the

samples were then vortexed, creating new supernatant suspensions of much higher concentrations. These samples were then consolidated in one or two 50 mL vortex tubes and centrifuged for the last time at 3000 rcf. Once more, most of the supernatant was removed and the samples were vortexed. The remaining, highly concentrated suspensions were transferred to aluminum weighing dishes and heated in a 60 °C oven for 1 day to remove any remaining water and recover the solid photocatalyst. The recovered photocatalyst was then crushed into finer particles using a mortar and pestle. This crushed catalyst was placed inside an RF plasma etcher (Harrick Plasma, USA) and air plasma was used to etch off the inactivated biomaterial that remained on the surface of the catalyst, i.e., regenerating the catalyst.

Brunauer, Emmett and Teller (BET) analysis was employed to determine the specific surface areas of various photocatalysts employed in this study. For the BET analysis, the nitrogen adsorption-desorption isotherms were recorded at a bath temperature of 77.25 K using a micromeritics ASAP 2020 Plus instrument. A JEOL JSM-7500F FE-SEM microscope was used to study the morphologies of the photocatalysts before and after their use in *E. coli* inactivation. A Jenway 6705 UV/Visible scanning spectrophotometer was used to obtain Ultraviolet-Visible (UV-Vis) spectra of the photocatalyst suspensions.

3.5. Mycometer Calibration

A large-scale UV-A photocatalytic disinfection experiment was performed to obtain a calibration for the BQ value (a calculated value based on proprietary formula

from Mycometer BactiQuant®) obtained from the Mycometer BactiQuant® water setup with respect to the number of colony forming units per volume over a wide range of cell concentrations. The experiment was performed in a similar manner as the large-scale UV-A photocatalytic disinfection experiment outlined above, with some modifications. A 100 mL sample was taken every 30 minutes to be quantified using the Mycometer, along with the aliquots taken for quantification of colony forming units using traditional spiral plating method.

In brief, the procedure utilized for the estimation of cell counts using the BQ value as a representative measure was as follows. The 100 ml water sample containing titanium dioxide as well as *E. coli* was passed through a syringe filter. This filter is then saturated with a proprietary substrate from the BactiQuant® Water kit. Following this, the soaked filter was allowed to rest for 30 minutes. The filter was then rinsed with the developer solution from the BactiQuant® Water kit and fluorescence measurements were taken. These measurements were converted to a quantitative measure of cell counts (the BQ value) using a proprietary formula after adjusting for the temperature of the environment and dilution factors, etc. A calibration data set was developed using the BQ values as well as the CFU/ml values from spiral plating performed in parallel.

This experiment could not be performed in conjunction with the regular UV-A photocatalytic disinfection experiment reported above, as taking 100 mL of volume out of the reactor every 30 minutes would change the residence time and have an effect on the overall kinetics of the disinfection.

3.6. Microorganism Growth for Small-Scale Experiments

Aliquots of *Escherichia coli* (QC101) preserved in glycerol stock at -80 °C were transferred into 50 mL of nutrient broth (LB Broth Miller) aseptically. The culture was then moved into a 37 °C incubator and slowly shaken using an orbital shaker for 18-20 hours. Four 1 mL samples of the culture were taken and placed in 1.5 mL centrifuge tubes. These samples were washed using the same procedure outlined previously, except a different centrifuge was used at 10000 rcf for 1 minute. After three washes, the samples were moved into a 10 mL vortex tube and Nanopure water was added until the final volume reached 10 mL, creating a resuspension of ~10^8 CFU/mL.

3.7. Small-Scale UV-A Disinfection Using Regenerated Catalyst

30 mg of the regenerated catalyst was added to 29.7 mL of Nanopure water within a quartz beaker. This mixture was then mixed for at least 2 hours. An aliquot (0.3 mL) of the *E. coli* resuspension was added to the nanowire suspension and allowed to mix for at least 15 minutes. For each photocatalysis run, the beaker was placed within 2.54 cm of the UV-A light source (SunLite® 20 W, 15 Lumens Blacklight). The light source and the sample were placed within a cardboard box with the inside covered in aluminum foil. All samples were continuous mixed for the duration of the experiment. 500 μL samples were drawn at pre-determined time intervals. Serial dilutions were performed as needed, vortexing each dilution to ensure complete mixing.

3.8. Measuring Dark Repair after Photocatalysis

Experiments were performed to understand the effect photocatalytic inactivation of *E. coli* has on their ability to reactivate through dark repair. The regrowth experiment was performed using the small-scale experiment setup. This experiment had three different samples, UV-A and nanowire (UV-A + NW), UV-A only (clear control), and nanowires only (dark control). To account for the larger sample volumes taken, the initial volume of Nanopure water added to the reactor was 40 mL. To this volume, 40 mg of porous TiO_2 nanowires were added and mixed for at least 2 hours. Nanowires were not added to the clear control sample. The bacteria resuspension was created identically to previous small-scale experiments, and was added to the nanowire suspension and mixed for at least 15 minutes. After proper mixing was achieved, three 5 mL samples were taken from each beaker and transferred to 15 mL vortex tubes covered in foil. These were the non-irradiated, or time = 0, samples. The UV-A + NW sample and the clear control were irradiated for 120 minutes by the UV-A light. The dark control sample was placed under a cup and covered in foil. All samples were continuously mixed for the duration of the experiment. After 120 minutes, three 5 mL samples were taken from each beaker and transferred to 15 mL vortex tubes covered in foil. These were the post-irradiation, or time = 120 minutes, samples. Aliquots from all six samples were plated using the same methodology outlined above. The samples were then stored in a 25 °C incubator and additional samples were taken and plated after 1, 3, and 5 days.

4. RESULTS AND DISCUSSION[*]

4.1. Large-Scale Disinfection Setup Performance

This section includes the results of all experiments using the large-scale system setup.

4.1.1. Kinetics of Large-Scale Disinfection Setup

The kinetics of *E. coli* inactivation in the benchtop system when Aeroxide® P25 nanoparticles and porous TiO_2 nanowires were employed as photocatalysts are depicted in Figure 2. Due to the dimensions of the purifier and inlet tank, the time variable is scaled by a factor of 40%. This additional calculation was performed because the purifier has a volume of ~2.75 L, while the required suspension volume to operate the flow system is ~7 L. This results in the suspension spending ~40% of the time within the reactor being irradiated, and the rest flowing throughout the system, mostly in the inlet tank. Using a scaled time allows for a better comparison with the small-scale experiments, as well as demonstrating what an ideal disinfection system, one without so much dead time spent traveling throughout the system, would produce.

The experiments indicated that over 97% reduction in *E. coli* CFU is possible with an exposure time of 100 minutes when porous TiO_2 nanowires were employed as the photocatalyst. A faster, approximately 3-log, reduction in *E. coli* in a span of 50 minutes

[*] Parts of this section are reprinted with permission from Bockenstedt, J., et al., *Catalyst Recovery, Regeneration and Reuse during Large-Scale Disinfection of Water Using Photocatalysis.* Water, 2021. **13**(19).

is possible when Aeroxide® P25 nanoparticles were employed for the photocatalysis. In both cases, the concentration of the photocatalysts in water was 0.1 g/l.

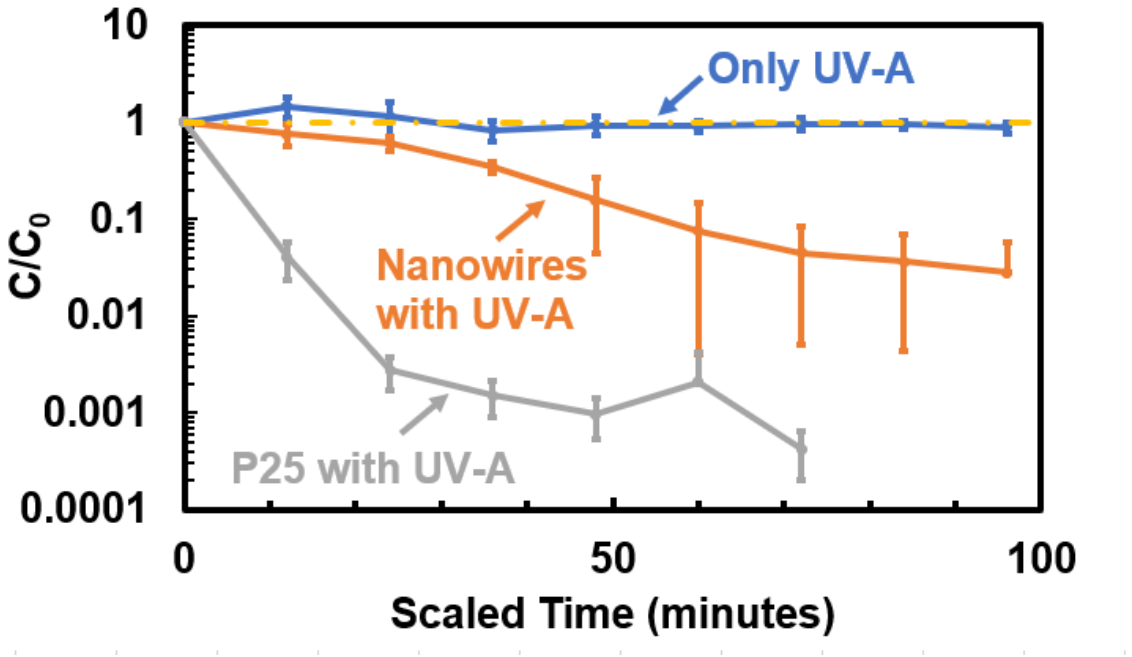

Figure 2 – *E. coli* inactivation in the benchtop water disinfection system built for 15.14 liters (4 gallons) of water per minute. The plot indicates that Aeroxide® P25 nanoparticles exhibit faster disinfection kinetics relative to that obtained using TiO2 porous nanowires. The photocatalyst concentration in both the cases was 0.1g/L. The errors bars represent the standard deviation calculated using a set of three trial runs.

These kinetics of *E. coli* inactivation were similar to those obtained when small-scale experimentation that involved the use of quarts beakers as photocatalysis reactors were employed [28] (Figure 3). As shown in Figure 3, three different controls were employed in the small-scale studies. Exposure of *E. coli* in water to only UV-A light

served as one control (clear control). The use of photocatalysts mixed with *E. coli* in water, without any UV-A activation of nanowires, served as a second control (dark control). Negative control involved the use of no photocatalysts and no UV-A exposure to *E. coli* suspended in water. All the controls indicated that the presence of both UV-A light and the photocatalysts is necessary for *E. coli* inactivation. The results of the clear control experiment on the benchtop experiment (Figure 2) indicate the behavior is consistent with that of the small-scale experiments.

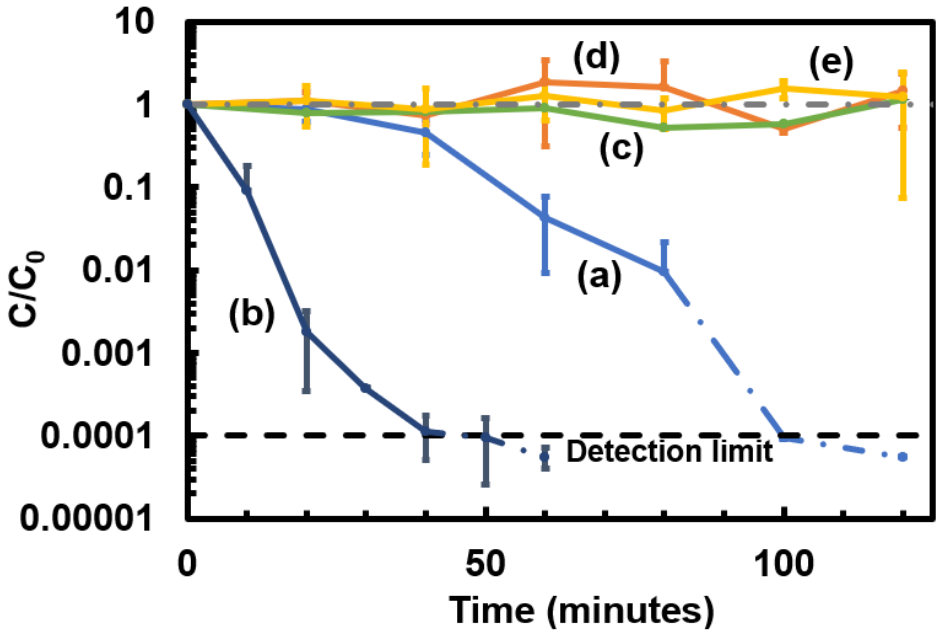

Figure 3 - A plot indicating the kinetics of *E. coli* inactivation in the beaker-scale water disinfection system. The letters in the plot indicate the following experimental conditions: (a) the disinfection kinetics of *E. coli*, using porous titanium dioxide nanowires as photocatalyst under exposure to UV-A light (b) the disinfection kinetics of Aeroxide® P25 nanoparticles under exposure to UV-A light (c) control case of a suspension of *E. coli* bacteria under exposure to UV-A light (d) a control case of suspension of E. coli bacteria and porous titanium dioxide nanowires without any UV-A light (e) a control case with a suspension of *E. coli* bacteria stirred for the duration of the experiment. The photocatalyst concentration in all the relevant cases was 1 g/L. The errors bars represent the standard deviation calculated using a set of three trial runs. The detection limit is the lowest concentration we can measure and any value below that is hypothetical and represented by a dashed line.

These results are also in agreement with the disinfection kinetics reported in literature. As can be seen in Figure 4, previous reports of photocatalytic disinfection of *E. coli* using TiO_2 nanoparticles as catalyst show inactivation kinetics ranging from 3 orders of magnitude decrease in CFU in two hours to a significantly faster 7 orders of magnitude

decrease in CFU within 40 minutes depending upon the conditions of the experiment [29], [30], [31], [32], [33], [34], [35]. The results from the small-scale experiments as well as on benchtop setup fit well within this range, for both the Aeroxide® P25 nanoparticles and the porous TiO2 nanowires. The wide range in kinetic data as shown in Figure 4 is likely a result of the varying experimental conditions, including catalyst concentration, the intensity of the UV-A radiation, and the reactor geometry. The study of the photocatalytic disinfection process at multiple scales, as shown in this work, will be useful in developing more holistic models for photocatalytic disinfection kinetics [36]. The studies referenced in Figure 4 as well as the current work investigate the disinfection kinetics in isolation, as they study the inactivation rates of *E. coli* in absence of any other contaminants in the water. Since photocatalytic disinfection of water from actual ground and surface water sources, as well as wastewater, needs consideration of the effects of total organic carbon (TOC) levels and the presence of various salts in water as reported by Abidi *et al.* [37], Moncayo-Lasso *et al.* [38], and Birben *et al.* [39]. However, such studies need to be performed on a large scale to better understand the challenges of scaling-up the photocatalytic disinfection process.

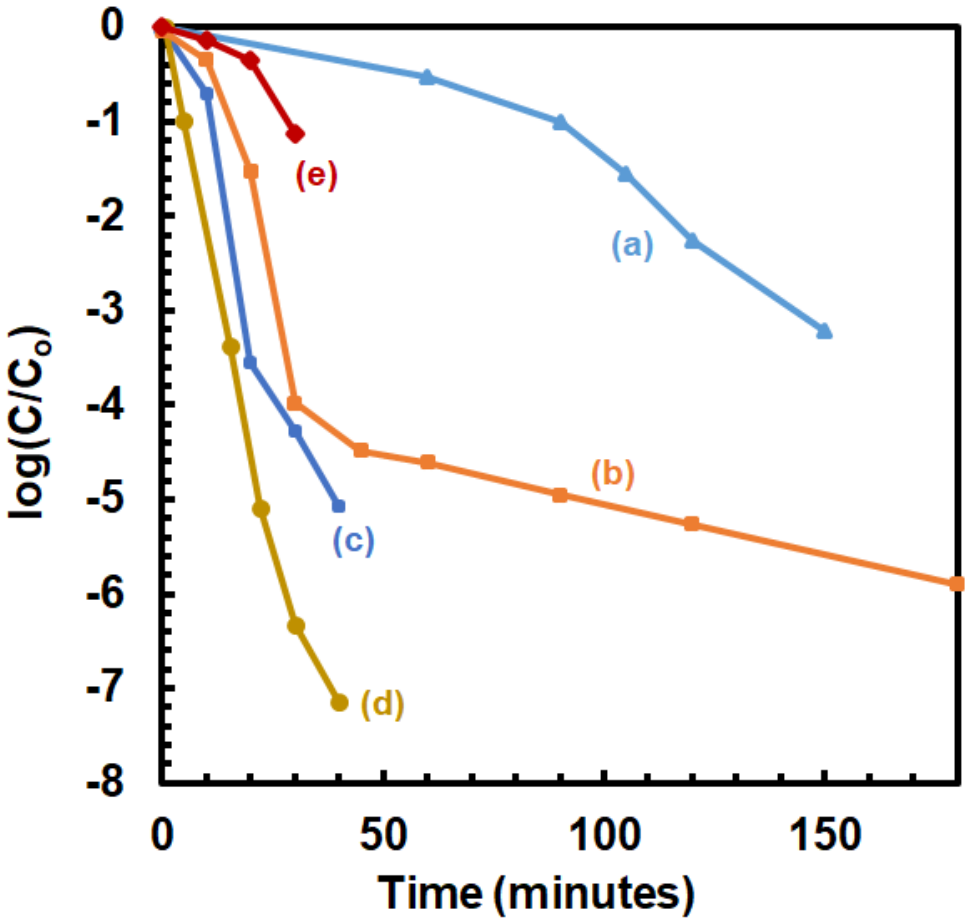

Figure 4 - Comparison of kinetics for the disinfection of *E. coli* using TiO2 Aeroxide® P25 as the photocatalyst activated using the following light sources. (a) 18-W black-light blue lamps [30], (b) irradiation produced by an HPK 125 lamp [29], (c) irradiation produced by a high intensity long-wave (highest emission at 365 nm) ultraviolet lamp [31], (d) irradiation produced by a solar simulation irradiation from a Hanau Suntest (AM1) lamp [35], (e) irradiation produced by 40-W black light tubes [33].

The lower rates of inactivation of *E. coli* in the presence of photoactivated porous TiO_2 nanowires relative to those observed with Aeroxide® P25 nanoparticles is believed to be because of the lower specific surface areas of the porous TiO_2 nanowires, as well as the lack of access to the surface sites for bacterial inactivation due to the nanoporous nature

of the nanowire surfaces (the surfaces have pores of sizes on the order of a few nanometers) [28]. Surface area analysis by Brunauer-Emmett-Teller (BET) method indicated that porous TiO_2 nanowires have a specific surface area of 26.11 m^2/g, lower than the 50-60 m^2/g of Aeroxide® P25 nanoparticles. The changes in the surfaces areas and the morphologies of the two photocatalysts is also believed to have led to differences in the magnitudes of the UV-A light absorbed, and this manifested as differences in the rates of *E. coli* inactivation of the two different photocatalysts. UV-Vis absorption spectra (Figure 5) for 0.05 g/L suspensions of both the porous TiO_2 nanowires and the Aeroxide® P25 TiO_2 nanoparticles indicated that they both absorb UV-A light. It is essential to add here that lower concentrations of the photocatalysts was employed for the UV-Vis study, as higher concentration did not allow for obtaining any discernible transmission of light for obtaining the UV-Vis spectra. In all, the studies indicated that efficiencies of photocatalytic disinfection of was achieved using small-scale experimentation are replicable in a benchtop setup and that it is possible to accomplish the continuous disinfection of water using photocatalysis.

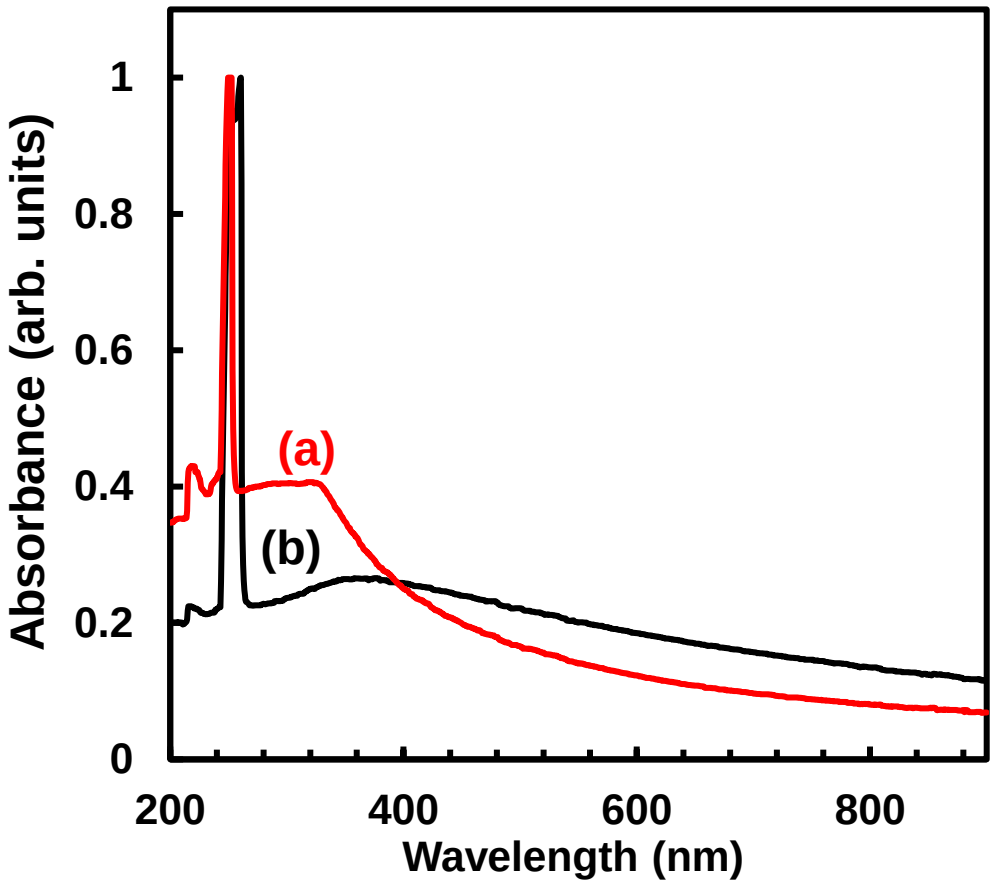

Figure 5 - UV-Vis absorption spectra for (a) TiO_2 Aeroxide® P25 nanoparticles and (b) TiO_2 porous nanowires. Both the spectra indicate light absorbance in the UV-A regime (i.e., 315-400 nm wavelength range). The relative differences in the magnitudes of UV-A absorbed could be attributed to the differences in both the morphologies and the surface areas of the two different types of the photocatalysts. The concentration of the photocatalysts used for this UV-Vis study was 0.05 g/L.

4.1.2. Mycometer Calibration

The calibration data set developed using the BQ values and the CFU/mL values from spiral plating performed in parallel was plotted to develop a calibration curve as shown in Figure 6. The Mycometer allows for rapid quantification of bacteria within

samples of water, and this calibration curve allows users to quickly convert the BQ values derived from the Mycometer into the more traditional CFU/mL values.

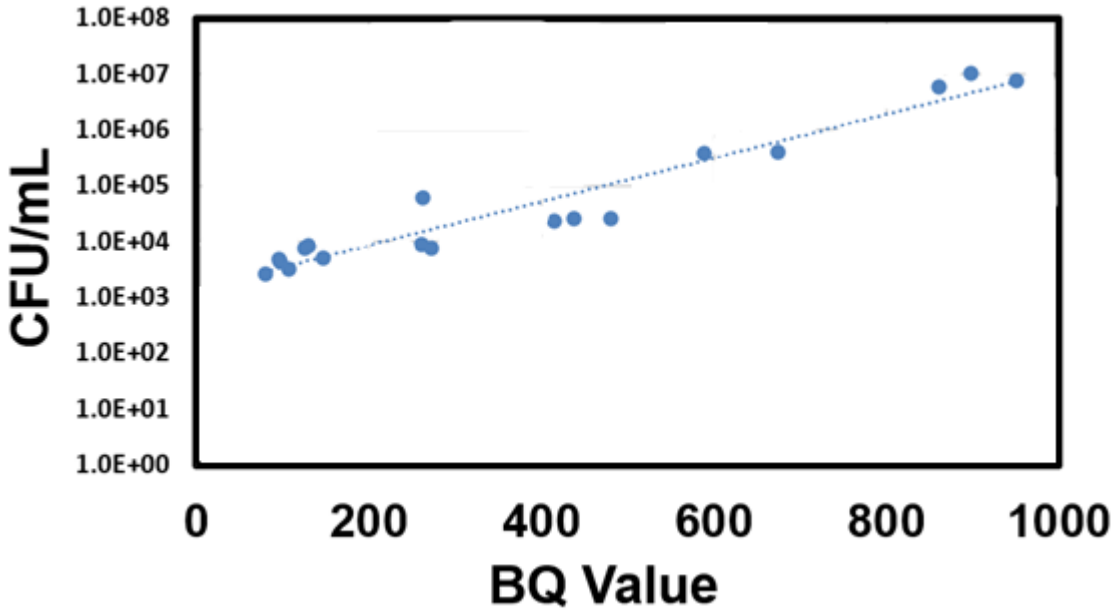

Figure 6 – Calibration curve developed using the BQ values (a calculated value based on proprietary formula from Mycometer BactiQuant®) and the CFU/mL values from spiral plating performed in parallel. Experiments were performed in triplicate to get results.

4.2. Recovery and Regeneration of Photocatalyst

Following the photocatalytic disinfection experiments, the wastewater was collected and treated using the methods outlined previously in this document. After the catalyst was ground using a mortar and pestle, the resulting powder was weighed. Overall, 77% of the Aeroxide® P25 nanoparticles and 57% of the TiO_2 porous nanowires were

recovered in our experiments. Further optimization of the process, including the use of in-line centrifuges, could be employed to recover a majority of the photocatalysts in a continuous manner from continuous flow-based photocatalytic reactors.

BET surface area analysis of the recovered and regenerated photocatalysts was performed to document surface area changes in the recovered and regenerated photocatalysts. In the case of nanoparticles, agglomeration and/or surface area contamination reduced the surface area from 50-60 m^2/g to 32.97 m^2/g. Upon plasma cleaning of the recovered Aeroxide® P25 nanoparticles, the available surface area increased from 32.97 m^2/g to 40.06 m^2/g. However, in the case of porous TiO_2 nanowires, the surface area of the recovered nanowires was estimated to be 25.09 m^2/g, much closer to that of the original nanowires of 26.11 m^2/g. The plasma regeneration of the surfaces in this case only resulted in a negligible increase in the available surface areas from 25.09 m^2/g to 25.14 m^2/g. This clearly indicates that agglomeration and loss of surface area is not a major problem in anisotropic shaped photocatalysts, such as nanowires, and that the recovery and regeneration of the photocatalysts is possible.

4.3. Regenerated Photocatalyst Disinfection Performance

Of key interest is the determination of the efficacy of the recovered photocatalyst. Experimentation performed to determine the kinetics of disinfection of the recovered and regenerated photocatalysts (Figure 7 and Figure 8) showed that as-recovered Aeroxide® P25 nanoparticles required a time of 60 minutes to achieve a three order of magnitude reduction in *E. coli*. Upon regeneration of the as-recovered catalyst with plasma treatment,

the photoactivity increased and led to a four order magnitude reduction of *E. coli* in the same 60-minute time span (Figure 7) The experimentation also indicated that as-recovered porous TiO_2 nanowires required a time of 120 minutes to reduce *E. coli* by one order of magnitude (Figure 8). Plasma cleaning of the as-recovered porous TiO_2 nanowires' surfaces for regenerating them aided in increasing the photocatalytic activity of the nanowires, leading to a two order decrease in *E. coli* in a span of 120 minutes. In both cases, the photoactivity of the regenerated catalyst in inactivating *E. coli* was lower than those of the respective original photocatalysts. However, the reduction in photoactivity was more pronounced for porous TiO_2 nanowires, relative to that observed in Aeroxide® P25 nanoparticles.

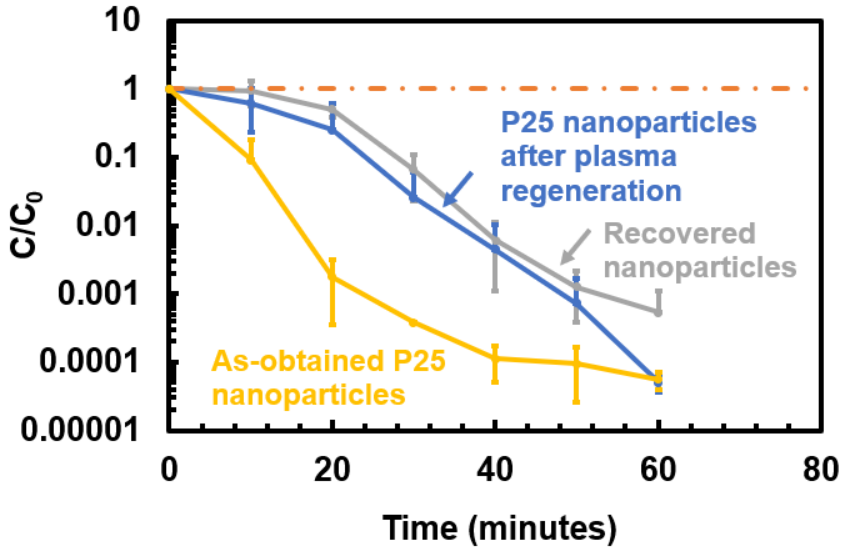

Figure 7 - Kinetics of *E. coli* disinfection in recovered and regenerated photocatalysts for Aeroxide P25® nanoparticles. The errors bars represent the standard deviation calculated using a set of three trial runs.

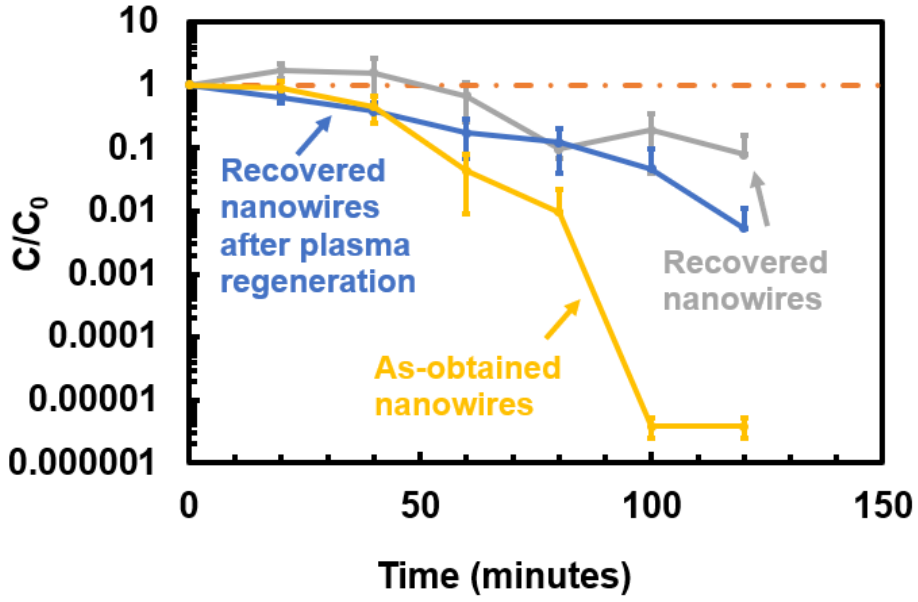

Figure 8 - Kinetics of *E. coli* disinfection in recovered and regenerated photocatalysts for TiO_2 porous nanowires. The errors bars represent the standard deviation calculated using a set of three trial runs.

This result is also supported by the morphology analysis of the TiO_2 porous nanowires before and after their use as photocatalysts (Figure 9). SEM micrographs of the TiO_2 porous nanowires before (Figure 9(a)) and after (Figure 9(b)) their use in photocatalysis indicated no major changes to the nanowire morphology or the nanowire dimensions. These results, combined with the BET analysis, further show that surface area loss is not a major problem in the nanowires, but it does not explain why the photoactivity of porous TiO_2 nanowires is lost upon recovery and regeneration. Further optimization of the plasma cleaning process, including using higher power plasmas for removing any

adventitious carbon on nanowire surfaces, is necessary to ensure that the photocatalysts is completely regenerated.

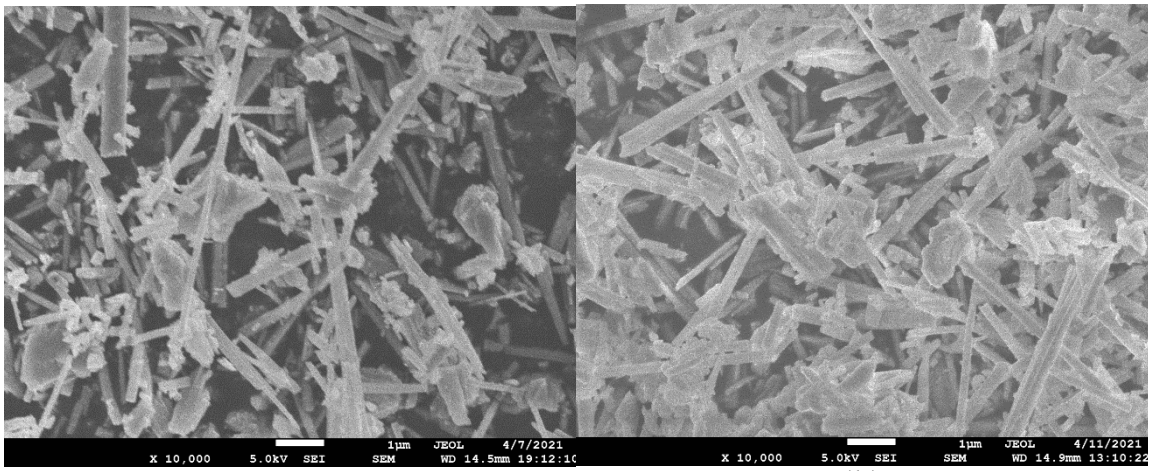

(a) **(b)**

Figure 9 - A comparison of morphologies of (a) as-obtained TiO_2 porous nanowires, and (b) TiO_2 nanowires recovered after photocatalysis. The micrographs indicate that the TiO_2 nanowires retain their morphology after their use as photocatalysts. This result is in line with the surface area analysis that indicated minimal change in the TiO_2 porous nanowire photocatalyst surface areas upon their use for *E. coli* inactivation in water.

4.4. Regrowth through Dark Repair

The intent of these experiments was to shed light on amount of time disinfection water could be stored before use, in the absence of any residual disinfection. In the following three figures (Figures 10-12), “Before treatment” indicates the concentration of *E. coli* in water samples that did not undergo any treatment, but aged in a similar manner as the treated samples.

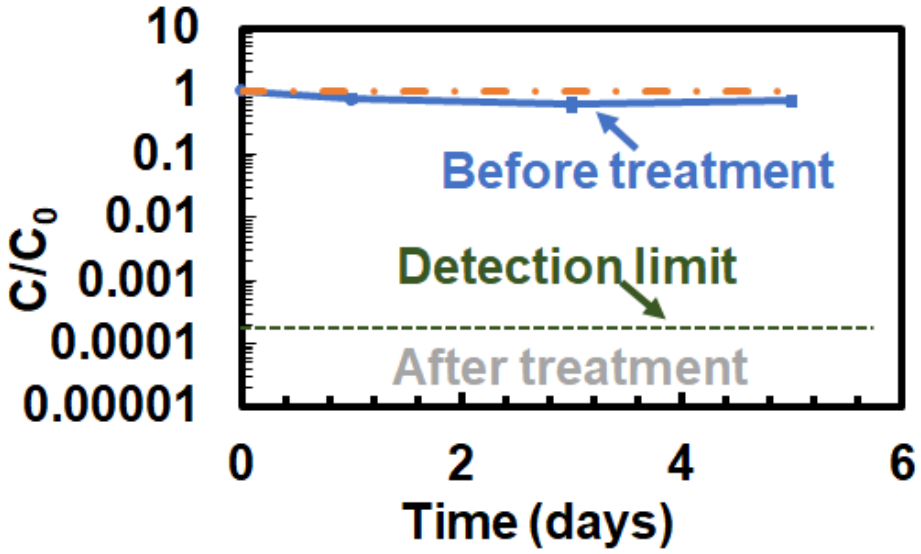

Figure 10 – Dark repair experimentation plot indicating the concentration of *E. coli* in water Vs. time the water was stored in the dark following treatment using photocatalysis with porous TiO_2 nanowires. The detection limit is the lowest concentration we can measure and any value below that is hypothetical and represented by a dashed line.

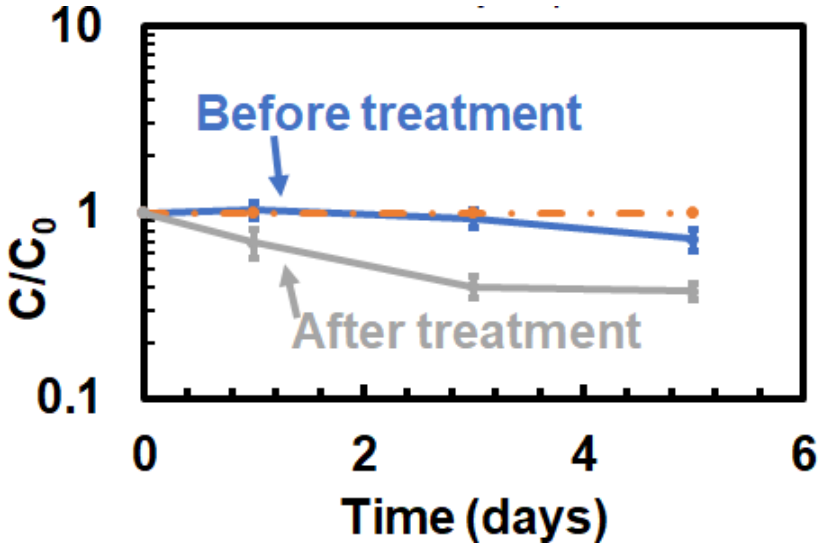

Figure 11 - Dark repair experimentation plot indicating the concentration of *E. coli* in water Vs. time the water was stored in the dark following exposure to nanowires that were not excited with UV light (dark control). The detection limit is the lowest concentration we can measure and any value below that is hypothetical and represented by a dashed line.

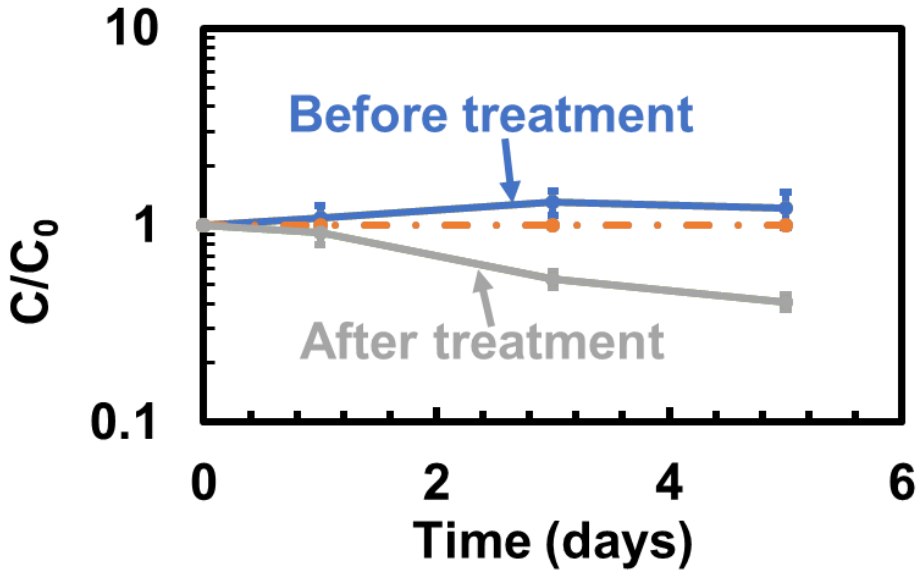

Figure 12 - Dark repair experimentation plot indicating the concentration of *E. coli* in water vs. time the water was stored in the dark following exposure to UV-A light in the absence of photocatalysts (clear control). The detection limit is the lowest concentration we can measure and any value below that is hypothetical and represented by a dashed line

As observed in Figures 11 and 12, slight reduction on the order of 1-long or lower was observed in both the dark and clear controls. Lack of growth media is believed to be responsible for this reduction in bacteria values. In sharp contrast, the *E. coli* concentrations remained below the detection limits in water treated by porous TiO_2 nanowires photocatalysts. These results clearly demonstrate that dark repair and reactivation of *E. coli* in water disinfected by photocatalysis did not occur within the 5-day storage period employed in the current study.

5. SUMMARY AND FUTURE WORK

5.1. Summary

Two major aspects associated with the development of photocatalysis as a process for the large-scale disinfection of water are addressed in this study, namely (a) the use of photocatalysis for processing large quantities of water, and (b) the recovery, regeneration, and reuse of the photocatalysts. The results indicated that the photocatalytic disinfection kinetics achieved by beaker-and-bottle experimentation are replicated in a benchtop system capable of processing 15.14 liters (4 gallons) of water per minute. The benchtop system built for this purpose is comprised of only commercially-available components, is mobile, and could be retrofitted into the water treatment trains currently used for processing wastewater. Moreover, experimentation in this study indicated that gravity-assisted settling, centrifugation, and air plasma surface cleaning could be used to recover and regenerate the photocatalyst for its subsequent use in disinfection additional quantities of water. Not only are the photocatalyst recovery and regeneration processes scalable, but also rapid. Such a rapid recovery and reuse of photocatalyst is critical for the deployment of photocatalysis as a process useful for water disinfection.

5.2. Future Work

Ideas and constructions presented in this document could be expanded upon to explore new pathways within the field. Some ideas for future work could include the following:

- The implementation of an in-line centrifuge within the large-scale unit to create a completely continuous disinfection system and testing the efficacy of the in-line centrifuge for photocatalyst removal.
- The use of ground, surface, or wastewaters sourced from local municipalities or utilities for determining how the total organic carbon (TOC) and salt levels affect the kinetics of disinfection.
- The recovery and regeneration of the same photocatalyst samples for multiple disinfection runs to determine the overall half-life of the photocatalysts.
- The use of the large-scale disinfection setup to purify water containing contaminants of emerging concern, such as pharmaceuticals.

REFERENCES

1. Drinan, J.E. and F. Spellman, *Water and Wastewater Treatment : A Guide for the Nonengineering Professional, Second Edition*. 2012, Baton Rouge, UNITED STATES: Taylor & Francis Group.

2. Villiers, M.d. *Water: The Fate of Our Most Precious Resource*. 2000.

3. Dieter, C.A., et al., *Estimated use of water in the United States in 2015*, in *Circular*. 2018: Reston, VA. p. 76.

4. ProQuest (Firm) and ebrary Inc., *Drinking water and health. Volume 2*. 1 online resource (xii, 393 pages).

5. *Wastewater technology fact sheet [electronic resource] : chlorine disinfection*, ed. W. United States. Environmental Protection Agency. Office of. 1999, Washington, DC: United States Environmental Protection Agency, Office of Water.

6. Morris, R.D., et al., *Chlorination, chlorination by-products, and cancer: a meta-analysis.* 1992. **82**(7): p. 955-963.

7. Stevens, A.A., et al., *Chlorination of Organics in Drinking Water.* 1976. **68**(11): p. 615-620.

8. Naumova, E.N., et al., *The elderly and waterborne Cryptosporidium infection: gastroenteritis hospitalizations before and during the 1993 Milwaukee outbreak.* Emerging infectious diseases, 2003. **9**(4): p. 418-425.

9. *Wastewater technology fact sheet [electronic resource] : ozone disinfection*, ed. W. United States. Environmental Protection Agency. Office of. 1999, [Washington, D.C.]: United States Environmental Protection Agency, Office of Water.

10. Langlais, B., D.A. Reckhow, and D.R. Brink, *Ozone in Water Treatment: Application and Engineering*. 2019: CRC Press.

11. Glaze, W.H.J.E.s. and technology, *Drinking-water treatment with ozone.* 1987. **21**(3): p. 224-230.

12. Von Gunten, U., Y.J.E.s. Oliveras, and technology, *Advanced oxidation of bromide-containing waters: bromate formation mechanisms.* 1998. **32**(1): p. 63-70.

13. Von Gunten, U., J.J.E.s. Hoigne, and technology, *Bromate formation during ozonization of bromide-containing waters: interaction of ozone and hydroxyl radical reactions.* 1994. **28**(7): p. 1234-1242.

14. Oguma, K., H. Katayama, and S. Ohgaki, *Photoreactivation of Escherichia coli after Low- or Medium-Pressure UV Disinfection Determined by an Endonuclease Sensitive Site Assay.* 2002. **68**(12): p. 6029-6035.

15. *Wastewater technology fact sheet ultraviolet disinfection*. 1999, United States Environmental Protection Agency, Office of Water: [Washington, D.C.] :.

16. Meulemans, C.C.E., *The Basic Principles of UV–Disinfection of Water.* Ozone: Science & Engineering, 1987. **9**(4): p. 299-313.

17. Morris, E.J.M.l.t., *The practical use of ultraviolet radiation for disinfection purposes.* 1972. **29**(1): p. 41-7.

18. Bolton, J.R. and C.A. Cotton, *The ultraviolet disinfection handbook*. 2008, Denver, CO: American Water Works Association.

19. Schneider, J., et al., *Understanding TiO2 Photocatalysis: Mechanisms and Materials.* Chemical Reviews, 2014. **114**(19): p. 9919-9986.

20. Dalrymple, O.K., et al., *A review of the mechanisms and modeling of photocatalytic disinfection.* Applied Catalysis B: Environmental, 2010. **98**(1): p. 27-38.

21. Foster, H.A., et al., *Photocatalytic disinfection using titanium dioxide: spectrum and mechanism of antimicrobial activity.* Applied Microbiology and Biotechnology, 2011. **90**(6): p. 1847-1868.

22. Mills, A. and S. Le Hunte, *An overview of semiconductor photocatalysis.* Journal of Photochemistry and Photobiology A: Chemistry, 1997. **108**(1): p. 1-35.

23. Hashimoto, K., H. Irie, and A. Fujishima, *TiO2Photocatalysis: A Historical Overview and Future Prospects.* Japanese Journal of Applied Physics, 2005. **44**(12): p. 8269-8285.

24. Jiménez-Tototzintle, M., et al., *Removal of contaminants of emerging concern (CECs) and antibiotic resistant bacteria in urban wastewater using UVA/TiO2/H2O2 photocatalysis.* 2018. **210**: p. 449-457.

25. Fagan, R., et al., *A review of solar and visible light active TiO2 photocatalysis for treating bacteria, cyanotoxins and contaminants of emerging concern.* 2016. **42**: p. 2-14.

26. World Health, O., et al., *Global solar UV index : a practical guide*. 2002, World Health Organization: Geneva.

27. Bockenstedt, J., et al., *Catalyst Recovery, Regeneration and Reuse during Large-Scale Disinfection of Water Using Photocatalysis.* Water, 2021. **13**(19).

28. Afreen, G., et al., *Bulk production of porous TiO2 nanowires by unique solvo-plasma oxidation approach for combating biotic and abiotic water contaminants.* Journal of Materials Science: Materials in Electronics, 2021. **32**(17): p. 21974-21987.

29. Benabbou, A.K., et al., *Photocatalytic inactivation of Escherischia coli: Effect of concentration of TiO2 and microorganism, nature, and intensity of UV irradiation.* Applied Catalysis B: Environmental, 2007. **76**(3): p. 257-263.

30. Cho, M., et al., *Different inactivation behaviors of MS-2 phage and Escherichia coli in TiO2 photocatalytic disinfection.* Applied and environmental microbiology, 2005. **71**(1): p. 270-275.

31. Ibáñez, J.A., M.I. Litter, and R.A. Pizarro, *Photocatalytic bactericidal effect of TiO2 on Enterobacter cloacae: Comparative study with other Gram (−) bacteria.* Journal of Photochemistry and Photobiology A: Chemistry, 2003. **157**(1): p. 81-85.

32. Khraisheh, M., et al., *Photocatalytic disinfection of Escherichia coli using TiO2 P25 and Cu-doped TiO2.* Journal of Industrial and Engineering Chemistry, 2015. **28**: p. 369-376.

33. Maness, P.C., et al., *Bactericidal activity of photocatalytic TiO(2) reaction: toward an understanding of its killing mechanism.* Applied and environmental microbiology, 1999. **65**(9): p. 4094-4098.

34. McCullagh, C., et al., *The application of TiO2 photocatalysis for disinfection of water contaminated with pathogenic micro-organisms: a review.* Research on Chemical Intermediates, 2007. **33**(3): p. 359-375.

35. Rincon, A.G. and C. Pulgarin, *Comparative evaluation of Fe3+ and TiO2 photoassisted processes in solar photocatalytic disinfection of water.* Applied Catalysis B: Environmental, 2006. **63**(3-4): p. 222-231.

36. Bloh, J.Z., *A Holistic Approach to Model the Kinetics of Photocatalytic Reactions.* Frontiers in chemistry, 2019. **7**: p. 128-128.

37. Abidi, M., et al., *Simultaneous removal of bacteria and volatile organic compounds on Cu2O-NPs decorated TiO2 nanotubes Competition effect and kinetic studies.* 2020.

38. Moncayo-Lasso, A., et al., *The detrimental influence of bacteria (E. coli, Shigella and Salmonella) on the degradation of organic compounds (and vice versa) in TiO2 photocatalysis and near-neutral photo-Fenton processes under simulated solar light.* Photochemical & Photobiological Sciences, 2012. **11**(5): p. 821-827.

39. Birben, N.C., C.S. Uyguner-Demirel, and M. Bekbolet, *Photocatalytic Removal of Microbiological Consortium and Organic Matter in Greywater.* Catalysts, 2016. **6**(6).